ORIGINAL PAPER

Highly conductive Poly(L-lactic acid) composites obtained via in situ expansion of graphite

Bai Xue[1] · Jianmin Ye[1] · Junhua Zhang[1]

Abstract In this work, highly electrically and thermally conductive biopolymer composites were prepared by low-temperature expandable graphite (EG) filling Poly(L-lactic acid) (PLLA) via an in situ exfoliation melt blending process. The electrical conductivity of the composites with various graphite contents was measured by a four-point probe resistivity determiner and a high value of 0.37 S/cm was obtained at 70 wt.% EG content. A hot-disk method was used to evaluate the thermal conductivity of the composites. At EG loading fraction of 70%, thermal conductivity of PLLA/EG composites reached to the highest 26.87 W/mK, which is 100 times higher than neat PLLA. The electrical percolation was observed in the vicinity of the thermal percolation threshold concentration. The expansion of EG was crucial to the overall conductivity of the blends, which was confirmed by X-ray diffraction (XRD) analysis and scanning electron microscope (SEM). Dynamic rheology analysis was applied to study the structural change by the interconnection of the exfoliated graphite flakes and the formation of the networks in the blends. Thermogravimetric analysis (TGA) was employed to determine the thermal properties of the investigated PLLA/EG composites.

Keywords Conductivity · Poly (L-lactic acid) (PLLA) · Networks · In situ expansion

✉ Junhua Zhang
zhangjh@scu.edu.cn

[1] The State Key Laboratory of Polymer Materials Engineering, Polymer Research Institute of Sichuan University, Chengdu 610065, China

Introduction

Recently, conductive polymeric composites which can be prepared by filling a polymer matrix with conductive fillers such as graphite, carbon black, graphene, carbon nanotubes, metal powers, etc. have been attracted a considerable research interest due to their superior properties such as highly electrical and thermal conductivity, good processing ability, weight advantage, low lost, and excellent resistance to corrosive environment [1–7]. Conductive polymer composites have a wide variety of industrial application such as positive temperature coefficient materials, corrosion-resistant materials, electromagnetic shielding, antistatic media, heat exchangers as well as environmentally sensitive membranes [4, 8–10].

Carbonaceous fillers appear to be the best promising fillers which are incorporated into polymers to improve the thermal and electrical conduction ability of the matrices. Carbonaceous fillers, like carbon fiber (CF) [11–13], carbon black (CB) [14, 15], graphite [16–18], and carbon nanotube [19, 20]; have ubiquitous advantages, such as light weight, intrinsic high conductivity, and most importantly cost-effective [6]. In recent years, many researchers have conducted to the processing of conductive polymer composites with graphitic fillers. Fina et al. [21] introduced graphite into immiscible polyvinylidene fluoride/maleated polypropylene blends to illustrate the current–voltage behavior of the composites and reached the conclusion that the composites with double-percolation structure showed enhanced conductivity compared with single-polymer composites containing the same graphite content. Nagata et al. [17] applied the percolation theory to investigate the influence of graphite shape and size on the electrical conductive properties of the blends which were obtained by incorporating polyethylene (PE) with both plate-like and spherical graphite.

Graphite, a naturally abundant material which consists of a layered structure with a c-axis lattice constant of 0.66 nm [17], is the most widely used conductive filler for the polymeric composites that maintain excellent corrosion resistance and hold highly electrical and thermal conductivity. The stacks of graphite flakes, known as graphene, are weakly bonded to each other by van der waals forces, which makes the intercalation of inserting agents possible [22, 23]. The superior properties such as excellent conductivity (10^6 S/m at ambient temperature [24]), generated from the natural graphite flakes, make graphite widely used in thermal and electrical management systems. Since there are no reactive ion groups on the graphite layers, the natural graphite must undergo the chemical intercalation to allow the polymer chains entering into the layers [25]. Graphite intercalation compound, known as expandable graphite (EG), can be rapidly expanded, to some extent, hundreds of times over its initial volume to form a wormlike morphology when subject to high temperature. Therefore, EG is widely used as a conductive additive in polymeric composites because of its intumescent property. The schematic illustrating the preparation of expanded graphite from natural graphite is shown in Fig. 1.

Generally, rather high fraction of the conductive filler within the polymers is needed to impart the resultant composites relatively high conductivity. The improvement in the electrical conductive abilities of the polymer composites increasing with an incremental fraction of conductive filler is observed in most composite systems. High stacking density of conductive filler within the matrices and then the formation of conductive networks lead to a significant increasement in electrical conductivity, which is explained by the percolation transition [26, 27]. However, the exfoliation of expandable graphite makes it easier to build 3 D-conductive networks that drastically increase the conductive properties of EG-containing blends, which demonstrates that markedly lower content of EG is able to reach the
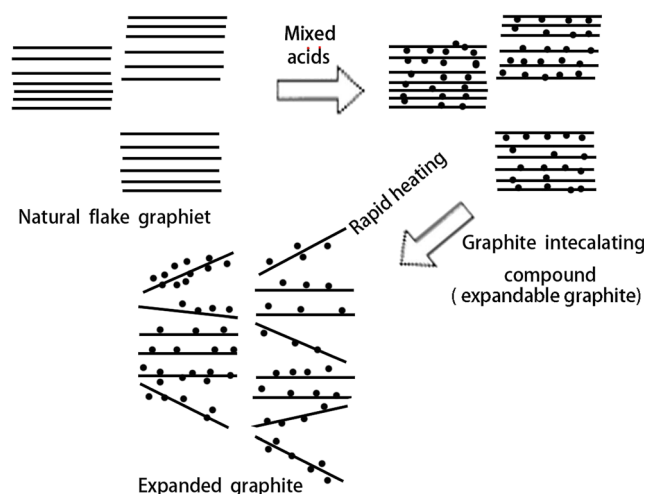
Fig. 1 A schematic showing the formation of expanded graphite from natural flake graphite

percolation threshold of conductivity in the EG-containing composites. Expanded graphite has a much higher volume expansion ratio than that of common graphite and exhibits a layered structure like layered silicates. The multi-pores, functional acids and the OH groups in the expanded graphite facilitate the affinity between the expanded graphite and the polymer matrix. Therefore, EG or expanded graphite is able to be incorporated into a variety of polymer matrices such as polyolefins, poly(-carbonate), polystyrene, polyurethane, poly(L-lactic acid), and so on, to enhance the electric and thermal conductivity and many other properties [28].

Poly(L-lactic acid) (PLLA) is one of the most extensively studied biodegradable polymers derived from annually renewable resources, and appears to be a promising material to alleviate the dependence on fossil fuels and to relieve solid waste disposal problems [29–32]. PLLA is a linear aliphatic thermoplastic polyester synthesized by the ring-opening polymerization of lactide and lactic acid which are prepared by the fermentation of sugar feed stocks [33, 34]. PLLA is a well-known bio-based material for its ideal combination of attractive properties such as good mechanical processability, renewability, biocompatibility, barrier, and transparency. A shortage of petroleum resources and environmental protection concerns open a brighter perspective for PLLA. It can be processed by a number of methods such as extrusion, compression molding, blow molding, injection molding, foaming, and fiber spinning, to yield articles to be applied in industrial packaging, drug delivery systems, surgical implants, and agricultural fields [35–38]. Moreover, PLA can be also used as the polymer matrix of the conductive polymer composites. To the best of our knowledge, the introduction of expandable graphite which owns much lower exfoliation temperature into the biodegradable PLLA matrix is rarely reported. It is believed that low-temperature EG can be fully exfoliated during the melt blending process of PLA/EG composites, which is crucial to the overall electrical and thermal conductivity of the composites.

In this article, a commercial grade low-temperature EG was incorporated into PLLA to prepare highly electrical and thermal conductive polymer composites. The conductivity of the composites increased with an incremental dosage of low-temperature EG and the percolation concentration was observed in the vicinity of 10 wt.%. The morphology and properties, such as crystalline, thermal stability properties, and rheological behavior of the composites were investigated.

Experimental

Materials

The PLLA (4032D) with a density of 1.24 g/cm^3 and molecular mass $M_w \approx 207$ kDa was purchased from Nature Works LLC (USA). PLLA presents a pellet form and consists of

about 2% D-lactide units. The commercial grade low-temperature expandable graphite (EG) with the trademark ADT KP251 and a size of about 300 μm was obtained from Shijiazhuang ADT Carbonic Material Factory (China). The sulfur-free EG with an initial expansion temperature in the vicinity of 150 °C is a kind of graphite intercalation compound which is obtained by the intercalation of acetic acid as the inserting agent. EG exhibits a density of 2.20 g/cm³ and the expansion ratio of 230 ml/g. It is used as the conductive filler as-received.

Sample preparation

Prior to blending, PLLA pellets were dried at 85 °C for at least 8 h in oven to remove eventual traces of moisture. And EG was also dried at 110 °C for at least 6 h. The PLLA/EG composites were obtained by simple mechanical blending. A composite system containing different fractions of EG was fabricated using Brabebder (Duisburg Germany) internal mixer at a screw speed of 30 rpm and at 180 °C for 8 min. Then, the samples used for measurements were compression-molded (HP-63D, Shanghai Zimmerli Weili Rubber & Plastic Machinery Co., Ltd, China) under the conditions of 10 MPa and at 185 °C and then cooled instantly under pressure to ambient temperature. Thus, a series PLLA/EG composites containing 0, 5, 10, 20, 30, 50, and 70 wt.% were obtained.

Measurements

Electrical and thermal conductivity measurement

The electrical conductivity of the PLLA/EG composites was measured by the four-point probe resistivity determiner (SIGNATONE, America) at room temperature. The hot pressed specimens were cut into dimensions of $40 \times 40 \times 4$ mm³ for testing. The electrical conductivity (σ) was obtained from the following equation:

$$\sigma = \frac{1}{\rho} = \frac{L}{RS} \tag{1}$$

Where ρ is the volume resistivity, R is the electrical resistance, S is the cross-sectional area, and L is the distance between clumps. Five tests were taken for the average value.

The thermal conductivity of the composites was determined using a thermal constant analyzer (Hot Disk TPS 2500, Sweden). The hot disk sensor with a radius of 3.189 mm was placed between two pieces of the obtained samples with a thickness of 4 mm. The whole unit of the sensor was clamped tightly and no silicone grease was used during the measurements. The thermal conductive value obtained in this measurement is a comprehensive value of all

directions. Each sample was tested 3 times and the average value was obtained.

X-ray diffraction analysis

To investigate the exfoliation of EG and the crystalline structure of the composites, X-ray diffraction (XRD) scans of the EG, expanded graphite, pure PLLA and PLLA/EG composites were carried out on a D/MAX-III X-ray diffractometer (DY1291, Philips, Holland) with Cu Ka radiation ($K=$ 0.1542 nm, 40 kV, 35 mA) in the scattering angle range of $2\theta = 5–40°$ at a scan speed of 0.06°/s.

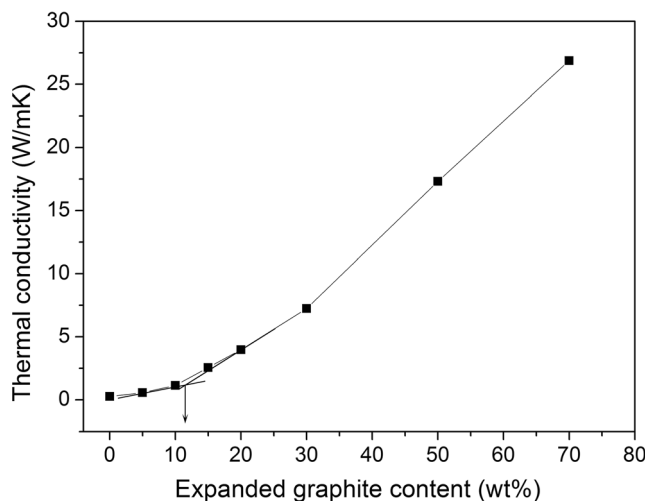### Morphology of PLLA/EG composites

The morphology of EG and PLLA/EG composites was observed by a scanning electron microscope (SEM; JSM-5900, JEOL, Japan) with an acceleration voltage of 20 kV. All the fractured surfaces of the samples which were cryogenically fractured in the liquid nitrogen were coated with gold to prevent electrostatic charging and to enhance the image resolution.

Dynamic rheological tests

Viscoelastic behavior of the composites was analyzed with the help of a dynamic rheometer (Bohlin Gemini 20,000, Malvern Instruments Ltd, UK) in the melt state. The samples were measured under a constant-strain mode. To keep the response in the linear viscoelastic region, the applied strain was set at 1% [39]. The samples in a parallel-plate form with a diameter of 25 mm and thickness of 1 mm were prepared by hot compression molding. All the specimens were test at 185 °C in a frequency sweep range from 0.01 to 100 HZ under nitrogen atmosphere. Elastic modulus (G') and loss modulus (G") of all of the samples were recorded as a function of angular frequency (ω).
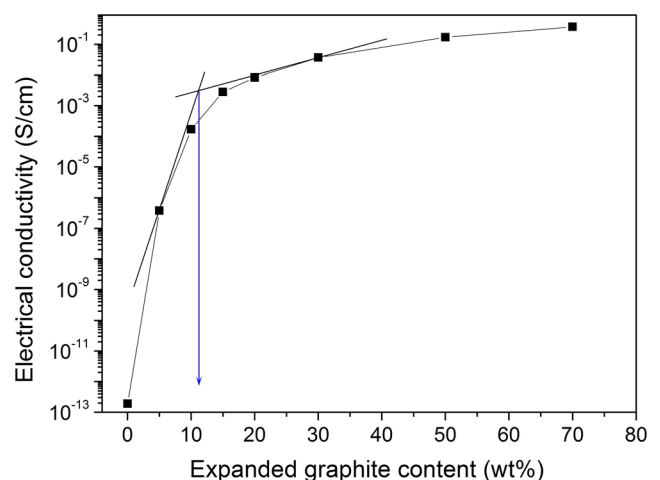
Fig. 2 Electrical conductivity of PLLA/EG composites as a function of expanded graphite content

Fig. 3 Thermal conductivity of PLLA/EG composites as a function of expanded graphite content

Thermogravimetric analysis

Thermogravimetric analysis (TGA) was conducted on a TGA analyzer (TA Q600, America) under a dry nitrogen atmosphere at a purge rate of 100 ml/min. The samples were heated from 30 °C to 600 °C at a heating rate of 10 °C/min. Both the residual weight and derived weight of the materials were recorded as a function of temperature in the heating process.

Results and discussion

Electrical and thermal conductivity

The effect of the loading fraction of expandable graphite (EG) on the electrical conductivity of the PLLA/EG blends is shown in Fig. 2. Like most polymers, PLLA is not an electrically conductive polymer. It is apparent that the electrical conductivity of the composites increases with the increasing EG content. The addition of EG drastically increases the conductivity of PLLA, with a sharp transition from an electrical insulator to a semiconductor.
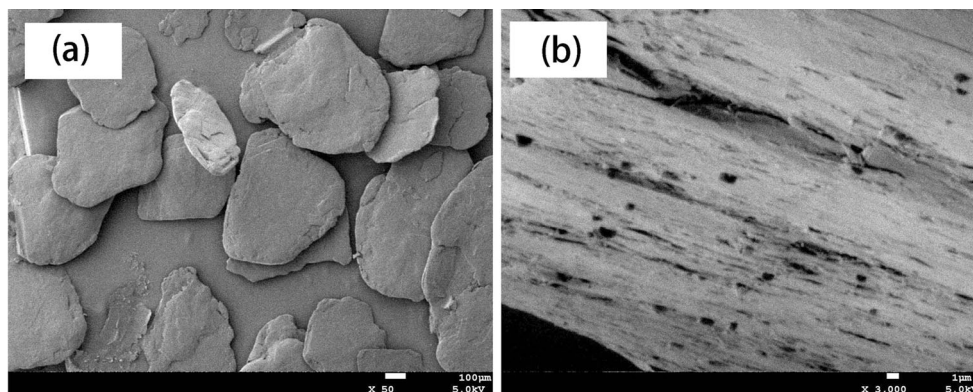
At the EG loading content of 15 wt.%, the conductivity of the composite is almost 10 orders of magnitudes higher than that of pure PLLA, which is attributed to the good dispersion of EG into the polymer matrix and the formation of conductive networks by graphite flakes exfoliated during the blending process. After EG loading fraction greater than 15 wt.%, the electrical conductivity of the composites augments slowly. Moreover, the electrical percolation threshold is clearly observed between 10 wt.% and 15 wt.%, or more specifically, at the graphite concentration of 11.9 wt.% in Fig. 2. The exfoliated graphite flakes could more easily form the connected networks in the composites than that of common graphite [3, 4]. The slow increase in the conductivity of PLLA/EG composites above 15 wt.% is mainly ascribed to the incremental number of interconnecting pathways built by the in situ exfoliated graphite flakes and the more compact structures rendered by the conductive filler.

The thermal conductivity values of PLLA/EG composites are plotted against the loading fraction of EG in Fig. 3. It is clearly seen that the thermal conductivity increases with an increasing weight fraction of EG up to 70 wt.%. The thermal conductivity of the composites is lower and increases slowly with the increasing EG loading content when less than 15 wt.%; the thermal conductivity begins to augment quickly after EG loading fraction greater than 15 wt.%. Basically, the conductivity increased slowly at low EG content is mainly due to the inadequate formation of interconnected networks by graphite flakes and high resistance generated from polymer matrix. As the EG loading concentration increased to 15 wt.%, the high expansion ratio of EG during the in situ expansion process leads to the formation of the heat conduction networks and the improvement of the effective volume of graphite flakes [40]. It is another crucial factor to the thermally conductive abilities of the PLLA/EG composites that a more compact structure rendered by the conductive filler is achieved with the increasing EG content.

A very highly thermal conductivity value of 26.87 W/mK versus 0.26 W/mK for the pure PLLA matrix is obtained for the PLLA/EG composite at the graphite loading of 70% by

Fig. 4 SEM images of EG at different magnifications: **a** 50× and **b** 3000 ×

Fig. 5 SEM micrographs of cryo-fractured surfaces of the PLLA/EG composites
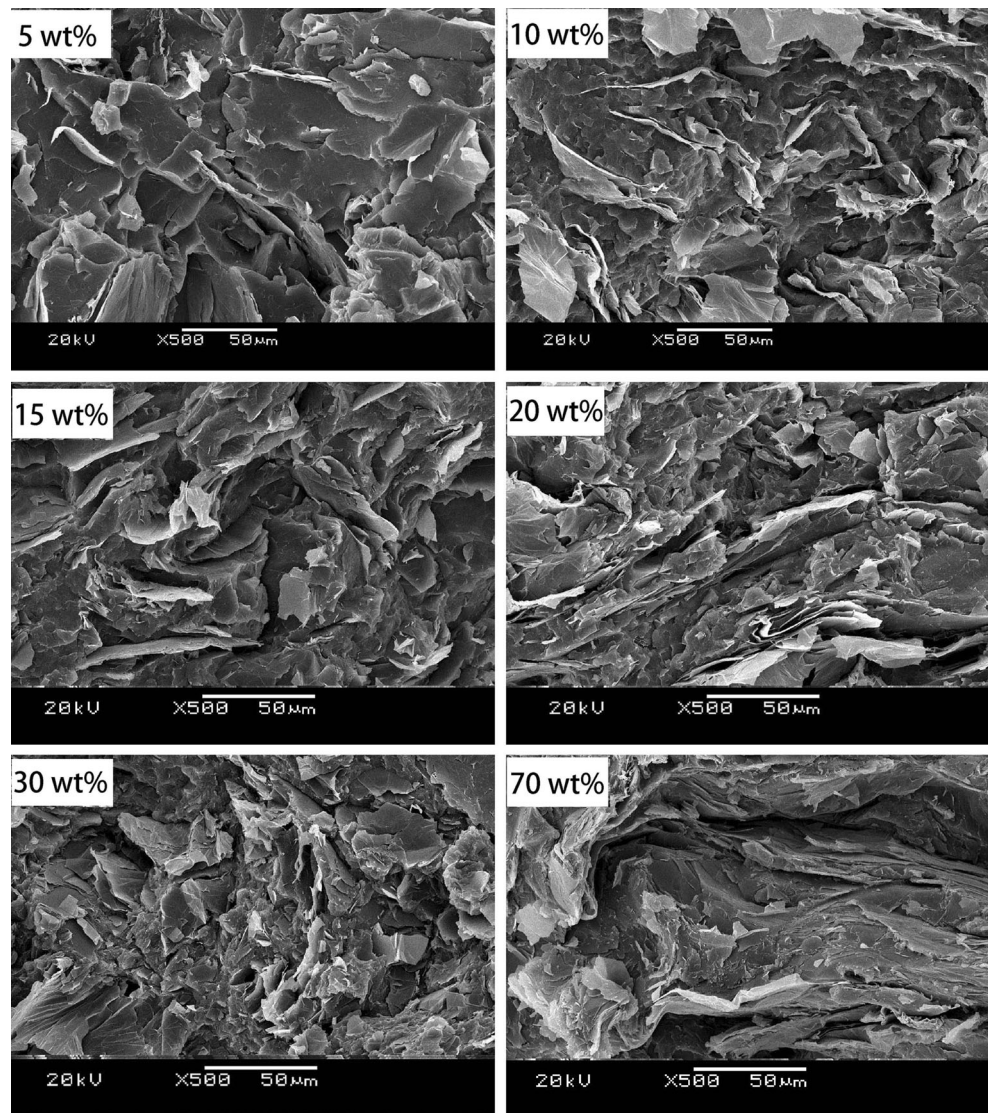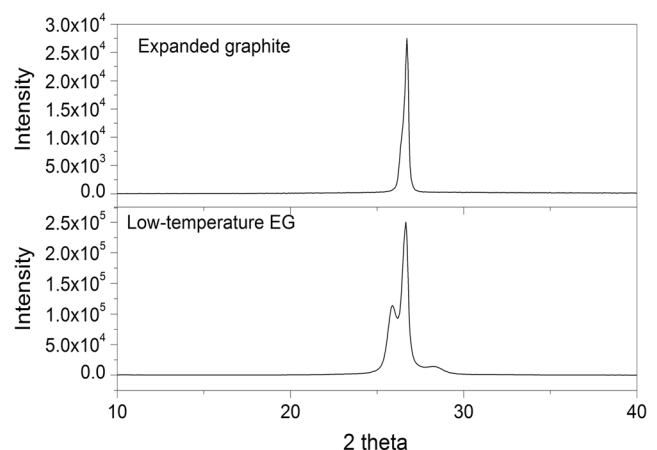

weight. Moreover, Fig. 3 also indicates that the thermal percolation threshold is observed at the graphite concentration of 11.5 wt.%, which is in the vicinity of the electrical percolation threshold concentration.
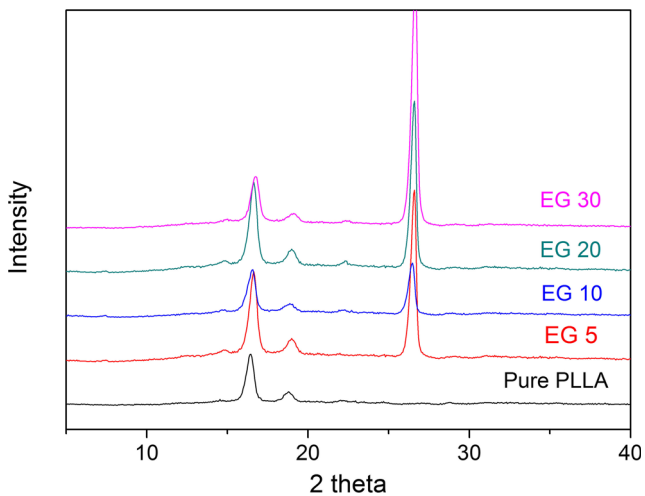
Morphology of the PLLA/EG composites

The SEM images of EG at different magnification is shown in Fig. 4. Representative micrograph Fig. 3a shows that almost all the EG particles exhibit a size of 300–400 μm. From Fig. 3b, it is clearly seen that EG consists of the stacking of a number of layers of graphite flakes which can be exfoliated during the blending process.

Figure 5 shows the morphology of the cryo-fractured surface of the PLLA/EG blends. It is illustrated that EG was well expanded during the melt blending process and the graphite flakes exfoliated from EG were evenly dispersed in PLLA matrix well. Specially, in Fig. 15 wt.%, the in situ exfoliated

graphite flakes begin to connect with each other and form the conductive networks in the blend, which demonstrates that the

Fig. 6 The XRD comparison patterns of expandable graphite and low-temperature expandable graphite
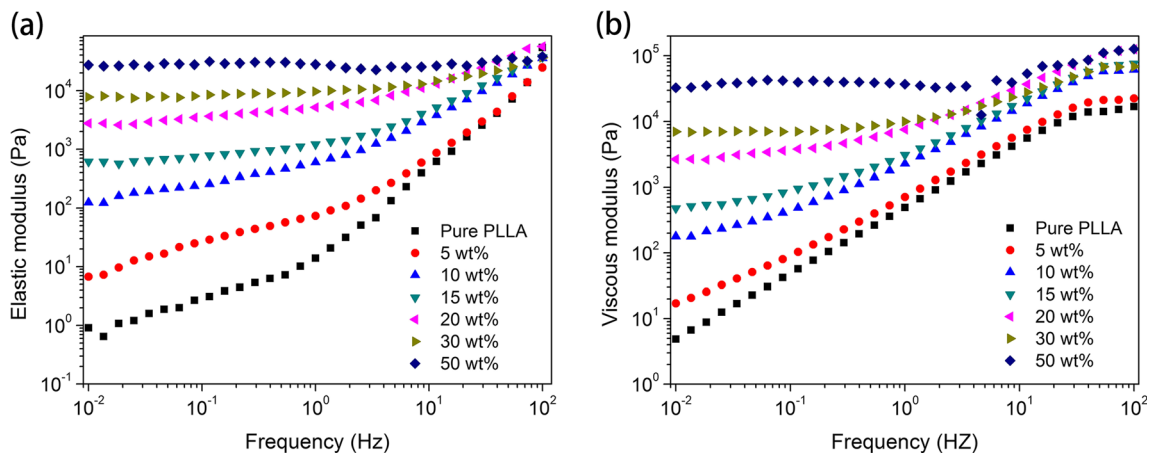
Fig. 7 The XRD comparison patterns of pure PLLA and PLLA/EG composites

X-ray diffraction analysis

XRD experiments were applied to investigate exfoliation of EG and crystal structure behavior of the PLLA/EG composites. Here, expanded graphite was prepared by rapidly heating EG at 700 °C for 5 min in a muffle furnace. The XRD patterns for expanded graphite and expandable graphite are shown in Fig. 6. It is observed that both samples exhibit a main strong characteristic peak at 2θ=26.5° which belongs to the crystalline form of the stacked graphite flakes [41]. An obvious shoulder peak at 2θ=25.8° is observed for the EG, belonging to a larger space between the graphite flakes which could be attributed to the intercalation of the inserting agents like acetic acid and concentrated sulfuric acid [42, 43]. The shoulder peak at 2θ=28.2° is related to the phase of graphite intercalated compound (expandable graphite) not to the amount of radicles in the gaps between graphite layers [43]. After heat treatment at 700 °C, the disappearance of the shoulder peaks is due to the escape of the inserting agents in EG, which is the main force driving the exfoliation process. It could be deduced from the variation of the intensity values that the crystalline form of EG is greatly improved by the expansion process [44].

The XRD patterns for pure PLLA and PLLA/EG blends are illustrated in Fig. 7. All the samples exhibited two typical diffraction peaks at about 2θ=16.5° and 18.9°, assigned to the (200)/(100) and (203) planes of the PLLA α crystal [45]. It is clearly seen that the introduction of EG into PLLA matrix has little effect on the crystalline forms of PLLA. However, the characteristic peak at 2θ=26.5° appears in the PLLA/EG composites, which is ascribed to the crystalline form deriving from the in situ exfoliated flakes. It demonstrates that the in situ exfoliated graphite flakes maintains well crystalline forms in the PLLA/EG composites. Moreover, compared with expandable graphite, the shoulder peaks at 2θ=25.8° and 28.2° related to the intercalation of the inserting agents is not observed for the PLLA/EG composites, which illustrates that the inserting agents have escaped from EG and graphite flakes

electrical and thermal conductivity of the composite system increases rapidly at the EG content of 15 wt.%. Moreover, a rather highly electrical conductivity of 2.8×10^{-3} S/cm is achieved at 15 wt.% EG content, which is nearly 10^{10} times higher than neat PLLA. The exfoliated graphite flakes are separated from each other and the conductive pathways are obstructed by the polymer matrix when the EG fraction is less than 15 wt.%. It is shown in Photo 20 wt.% that graphite flakes have already formed perfect conductive networks, and a more compact structure rendered by the conductive filler is achieved with the increasing EG content. Both factors are crucial to the electrical and thermal conductive abilities of the PLLA/EG composites. This is even more apparent in Fig. 30 wt.% and 70 wt.%. The electrical conductivity of the blends increases rapidly with the incremental EG content and its value reaches 0.37 S/cm at EG content of 70 wt.%, which is approximately 12 orders of magnitudes higher than that of pure PLLA, because the conductive networks have been perfectly built.
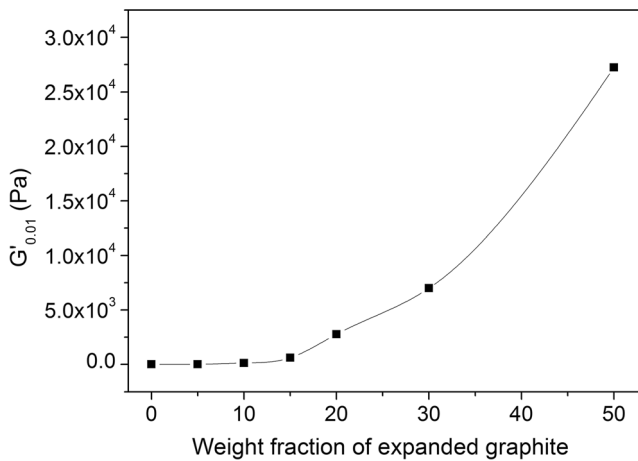

Fig. 8 **a** G' and **b** G" as a function of ω for different expanded graphite content for PLLA/EG composites

Fig. 9 Dependence of G' value at the ω of 0.01 HZ ($G'_{0.01}$) on the weight fraction of expanded graphite for estimating the critical weight fraction defined as percolation threshold

have been fully exfoliated. In combination with the morphology results, the exfoliation of EG is beneficial to the building of the conductive networks which is the crucial factor to the overall electrical and thermal conductivity of the composites.

Dynamic rheological tests

The dependence of elastic modulus (G') and viscous modulus (G") on angular frequency (ω) for the PLLA/EG composites is shown in log-log plots in Fig. 8, respectively. It is obvious that both G' and G" values of the composites which are sensitive to variations in composition and frequency increase with an increasing weight fraction of graphite up to 50 wt.% in the range of frequency employed. Magnitude of the modulus values increases with the increasing EG fraction at the low frequency regime and reaches the highest value at 50 wt.% EG content which is about 10^4 times higher than that of pure PLLA. However, the slopes of the curves decrease with the increasing EG fraction. Specially, a plateau is observed at the low frequencies after EG loading fraction greater than

10 wt.%. This is a famous phenomenon, known as the percolation threshold, which indicates the formation of a mechanically connected network by the fillers. The connected network formation which is mainly responsible for enhancing the conductivity of the composites is believed to result from the in situ exfoliation of EG during the melt blending process.

The identification of the percolation concentration (θ_c) can be carried out using the rheological data [4]. As shown in Fig. 8a, the elastic modulus becomes insensitive to frequency when the filler weight fraction reaches 15%. This indicates that the rheological behavior of the PLLA/EG composites changes from a viscous fluid to an elastic solid, which accompanies with the well formation of the conducting networks by exfoliated graphite flakes. That could be referred to the percolation threshold, which is the critical filler content when the connected network in the composites is formed by the fillers. In addition, the transition is observed exactly at the same composition in Fig. 8b which shows the plots of G" versus frequency.

The G' at the lowest frequency applied ($G'_{0.01}$) plotted against the weight fractions of EG graphite is shown in Fig. 9. Two distinct regions could be clearly seen on the curve and the turning point observed at which weight fraction of EG is defined as the percolation threshold for the blends [46]. It is also a very effective way to determine the structural change in the composition caused by the introduction of the organic fillers [47]. In combination with the electrical and thermal conductivity results, it could be concluded that the percolation threshold of the blends is near the concentration of 15 wt.% EG, or more specifically, between 10 and 15 wt.%.

Thermal stability analysis

The thermal decomposition and stability of pure PLLA and PLLA/EG composites were investigated by thermogravimetric analysis (TGA) under nitrogen atmosphere. The residual weight and derived weight thermograms as a function of
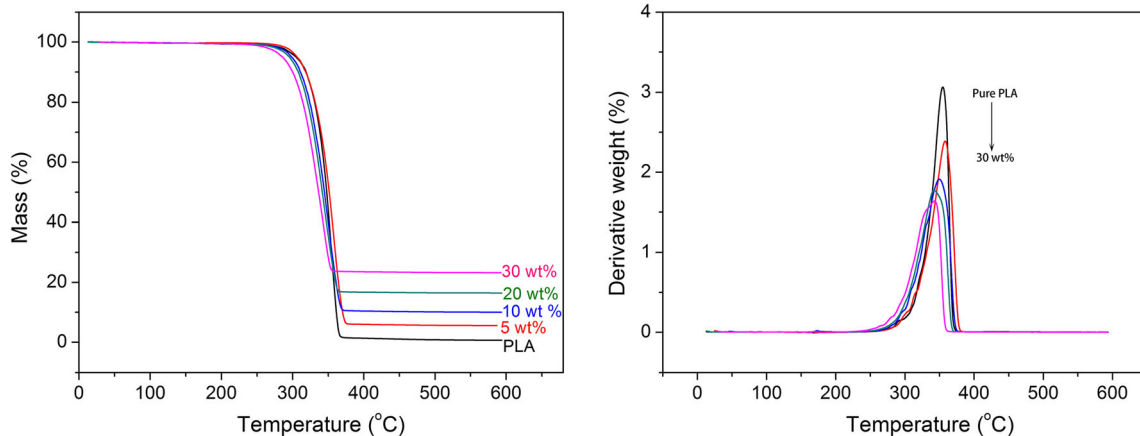
Fig. 10 TGA and DTG thermograms of the pure PLLA and PLLA/EG composites

Table 1 TGA T_d, T_{max}, and R_e values of the neat PLLA and PLLA/EG composites

EG content (wt%)	T_d(°C)	T_{max}(°C)	R_e (%)
0	332.3	354.6	0.65
5	330.3	358.0	5.56
10	318.7	349.8	10.00
20	313.8	342.1	16.44
30	306.1	342.6	23.22

temperature for PLLA/EG composites are shown in Fig. 10. The initial decomposition temperature (T_d), the maximum weight loss temperature (T_{max}), and the eventual residual weight percentage (R_e) are collected in Table 1. T_d is defined as the temperature at 5% weight loss, whereas T_{max} is taken from the peak value of the derivative thermogravimetry (DTG) thermograms. All of the TGA thermograms for the materials exhibit similar tendency. T_d slightly decreases with the increasing EG content, which indicates that the thermal stability of the blends deteriorates with the introduction of EG into PLLA matrix. However, T_{max} changes marginally and a higher value is obtained for the PLA/EG composite at the EG content of 5 wt.% than pure PLLA. This could be ascribed to the barrier effect of the exfoliated graphite flakes against the volatile pyrolyzed products [48]. Interestingly, T_{max} decreases with the incremental loading of EG in the blends after 5 wt.% EG content; its value was about 16 °C lower for 30 wt.% EG content than 5 wt.%. This phenomenon can be conjectured that (1) the in situ exfoliation of EG introduces a certain number of void defects, confirmed by the SEM images, and thus accelerates the decomposition process, (2) the inserting acid remained in the composites could catalyze the degradation of PLLA, and (3) the highly thermal conductivity of the blends facilitates the heat conduction into the interior of PLLA/EG blends, then degradation of the

composites could take place almost simultaneously inside and outside the composites.

Mechanical properties

The tensile tests were carried out on selected samples at room temperature, and the results are shown in Fig. 11. Both tensile strength and elongation at break of the PLLA/EG composites decrease with the increasing EG loading fraction. The most probable reasons for this phenomenon are as follows: (1) the inevitable aggregation of the filler results in more regions of stress concentration that require less energy to propagate the cracks, (2) the in situ exfoliation of expandable graphite introduces some void and crack defects, which is observed in the SEM images.

When added with 15 wt.% EG, higher than percolation threshold concentration, the resulting PLLA-based composites could lead to specific properties such as highly thermal and electrical conductivity while maintaining acceptable tensile strength of about 41.5 MPa.

Conclusion

In this study, highly electrically and thermally conducting Poly(L-lactic acid) (PLLA) composites with high loadings of low-temperature expandable graphite (EG) were achieved by an in situ exfoliation melt blending process. An electrical conductivity of 0.37 S/cm was obtained for the biodegradable PLLA/EG composites at its maximum filler content of 70 wt.%, which is about 10^{12} times higher than neat PLLA; at this EG loading fraction, thermal conductivity of PLLA/EG composites also reached to the highest 26.87 W/mK, which is 100 times higher than pure PLLA. In the present of EG, a percolation threshold reduction for the PLLA/EG composites
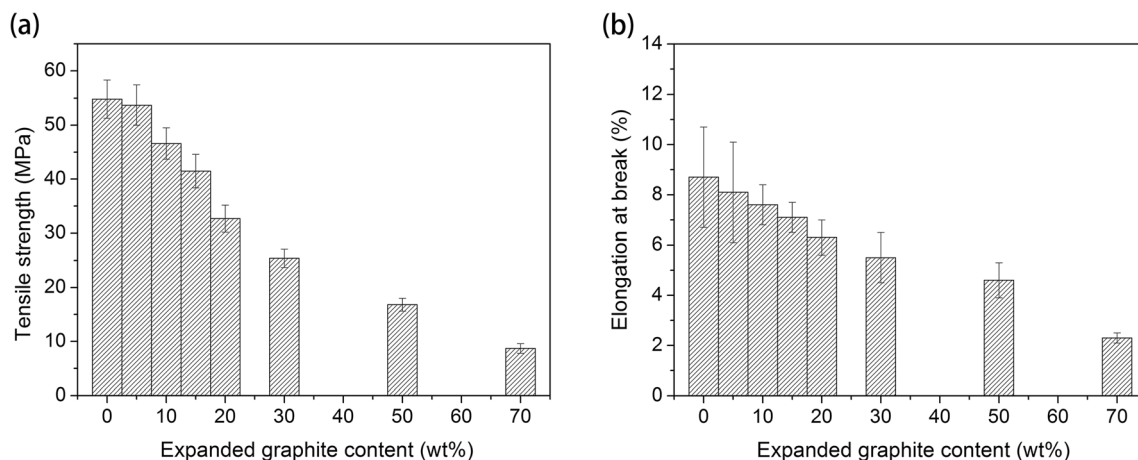
Fig. 11 **a** Tensile strength and **b** Elongation at break for PLLA composites with different contents of expanded graphite

was achieved, and the electrical percolation was observed in the vicinity of the thermal percolation threshold concentration. The in situ exfoliated graphite flakes could well form the conductive networks in the PLLA/EG composites, which was thought to be the main factor to the enhancement of conductivity properties of the composites. X-ray diffraction analyses confirmed the in situ exfoliation of EG during the melt blending process. The network formation by the exfoliated graphite flakes in the EG containing composites was confirmed by dynamic rheology measurements, which conformed to the SEM observations.

References

1. Chang J, Ho A, Chin WK (2007) J Polym Sci Part B Polym Phys 45:322–329
2. Luo Y, Liu Y, Yu Q (2007) Thin Solid Films 515:4016–4023
3. Zhou S, Chen Y, Zou H, Liang M (2013) Thermochim Acta 566:84–91
4. Zhou S, Lei Y, Zou H, Liang M (2013) Polym Compos 34:1816–1823
5. Kasgoz A, Akın D, Durmus A (2012) Polym Eng Sci 52:2645–2653
6. Han Z, Fina A (2011) Prog Polym Sci 36:914–944
7. Narkis M, Ram A, Flashner F (1978) Polym Eng Sci 18:649–653
8. Dai K, Xu XB, Li ZM (2007) Polymer 48:849–859
9. Zribi K, Feller JF, Elleuch K, Bourmaud A, Elleuch B (2006) Polym Adv Technol 17:727–731
10. Jouni M, Boudenne A, Boiteux G, Massardier V, Garnier B, Serghei A (2013) Polym Compos 34:778–786
11. Wu X, Qi S, He J, Chen B, Duan G (2010) J Polym Res 17:751–757
12. Agari Y, Ueda A, Nagai S (1994) J Appl Polym Sci 52:1223–1231
13. Shi SL, Zhang LZ, Li JS (2009) J Polym Res 16:395–399
14. Kim DJ, Seo KH, Hong KH, Kim SY (1999) Polym Eng Sci 39:500–507
15. Yi XS, Zhang JF, Zheng Q, Pan Y (2000) J Appl Polym Sci 77:494–499
16. Xue B, Feng T, Zhou S, Bao J (2014) J Poly Res 21:1–8
17. Gao JF, Yan DX, Huang HD, Zeng XB, Zhang WQ, Li ZM (2011) J Polym Res 18:2239–2243
18. Saleem A, Frormann L, Iqbal A (2007) J Polym Res 14:121–127
19. McCullen SD, Stano KL, Stevens DR, Roberts WA, Monteiro-Riviere NA, Clarke LI, Gorga RE (2007) J Appl Polym Sci 105:1668–1678
20. Villmow T, Pötschke P, Pegel S, Häussler L, Kretzschmar B (2008) Polymer 49:3500–3509
21. Fina A, Han Z, Saracco G, Gross U, Mainil M (2012) Polym Adv Technol 53:2412–2421
22. Uhl FM, Yao Q, Wilkie CA (2005) Polym Adv Technol 16:533–540
23. Lee Y, Kim D, Seo J, Han H, Khan SB (2013) Polym Int 62:1386–1394
24. Pan YX, Yu ZZ, Ou YC, Hu GH (2000) J Polym Sci Part B Polym Phys 38:1626–1633
25. Zhao YF, Xiao M, Wang SJ, Ge XC, Meng YZ (2007) Compos Sci Technol 67:2528–2534
26. Liu X, Wu Q (2002) Eur Polym J 38:1383–1389
27. Chiu HT, Hsiao YK (2006) J Polym Res 13:153–160
28. Yu J, Wang N, Ma X (2008) Biomacromolecules 9:1050–1057
29. Vainionpää S, Rokkanen P, Törmälä P (1989) Prog Polym Sci 14:679–716
30. Mehta R, Kumar V, Bhunia H, Upadhyay SN (2005) Polym Rev 45:325–349
31. He F, Li S, Vert M, Zhuo R (2003) Polymer 44:5145–5151
32. Leenslag JW, Pennings AJ, Bos RRM, Rozema FR, Boering G (1987) Biomaterials 8:311–314
33. Kricheldorf HR, Boettcher C, Tönnes KU (1992) Polymer 33:2817–2824
34. Lunt J (1998) Polym Degrad Stabil 59:145–152
35. Bos RRM, Rozema FB, Boering G, Nijenhius AJ, Pennings AJ, Verwey AB, Nieuwenhuis P, Jansen HWB (1991) Biomaterials 12:32–36
36. Penning JP, Dijkstra H, Pennings AJ (1993) Polymer 34:942–951
37. Penning JP, Grijpma DW, Pennings AJ (1993) J Mater Sci Lett 12:1048–1051
38. Fambri L, Pegoretti A, Fenner R, Incardona SD, Migliaresi C (1997) Polymer 38:79–85
39. Chen Y, Zou H, Liang M, Liu P (2013) J Appl Polym Sci 129:945–953
40. Ling W, Gu A, Liang G, Yuan L (2010) Polym Compos 31:307–313
41. Yasmin A, Luo JJ, Daniel IM (2006) Compos Sci Technol 66:1182–1189
42. Uhl FM, Yao Q, Nakajima H, Manias E, Wilkie CA (2005) Polym Degrad Stabil 89:70–84
43. Ying Z, Lin X, Qi Y, Luo J (2008) Mater Res Bull 43:2677–2686
44. Pötschke P, Fornes TD, Paul DR (2002) Polymer 43:3247–3255
45. Miyata T, Masuko T (1997) Polymer 38:4003–4009
46. King JA, Jhonson BA, Via MD, Ciarkowski CJ (2010) Polym Compos 31:497–506
47. Kasgoz A, Akın D, Durmus A (2012) Polym Eng Sci 52:2645–2653
48. Zhao YF, Xiao M, Wang SJ, Ge XC, Meng YZ (2007) Compos Sci Technol 67:2528–2534